

See discussions, stats, and author profiles for this publication at: <https://www.researchgate.net/publication/231671768>

# Photochemistry of colloidal semiconductors. 30. HPLC investigation of small CdS particles

ARTICLE *in* LANGMUIR · MARCH 1989

Impact Factor: 4.46 · DOI: 10.1021/la00086a024

---

CITATIONS

85

---

READS

32

4 AUTHORS, INCLUDING:



[Horst Weller](#)

University of Hamburg

391 PUBLICATIONS 27,015 CITATIONS

[SEE PROFILE](#)



[Lynne Katsikas](#)

Faculty of Technology and Metallurgy, Univer...

77 PUBLICATIONS 2,091 CITATIONS

[SEE PROFILE](#)

# Photochemistry of Colloidal Semiconductors. 30. HPLC Investigation of Small CdS Particles

Ch.-H. Fischer, H. Weller, L. Katsikas, and A. Henglein\*

Hahn-Meitner-Institut Berlin GmbH, Bereich Strahlenchemie, Postbox 39 0128,  
D-1000 Berlin 39, F.R.G.

Received July 29, 1988. In Final Form: November 10, 1988

HPLC is used to determine the size distribution of CdS colloids. These distributions agree with those obtained from electron microscopy. The method is applied to recognize "magic" agglomeration numbers and to follow thermal particle growth and photodissolution. In the thermal growth a gradual increase in size is ascribed to Ostwald ripening. However, in the beginning a rather abrupt increase in size takes place that is ascribed to particle combination. In the photodissolution of a sample containing two size distributions, the larger particles disappear more rapidly than the smaller ones, this effect being particularly pronounced when light of longer wavelengths is used where the small particles have little absorption.

## Introduction

Exclusion chromatography under normal pressure has been described in two papers as a method for the separation of small inorganic colloid particles of different size.<sup>1,2</sup> Such small particles often have photocatalytic properties,<sup>3</sup> more recently, their fluorescence,<sup>4</sup> size quantization effects,<sup>5</sup> and nonlinear optical properties<sup>6</sup> have been studied. In the present work, high-pressure liquid exclusion chromatography is used to analyze size distributions of CdS samples. HPLC has the advantage of short elution times, which allow one to study extremely small particles that grow fast. In addition, the resolution is better due to the smaller size of the grain of the stationary phase, and the analysis requires less solution. On the other hand, exclusion chromatography under normal pressure still seems to be an appropriate method when separation on a preparative scale is required.

The calibration of the column with various colloidal CdS samples of relatively narrow size distributions is described here. These distributions were determined by electron microscopy. It is shown that—once a column is calibrated—size distributions of unknown samples can be obtained by HPLC, these distributions being in good agreement with those from electron microscopy. HPLC experiments are also described in which the thermal growth and the photoanodic dissolution of CdS particles are observed.

## Experimental Section

The equipment consisted of a Merck-Hitachi pump, type L 6000, and a Waters photodiode array detector, type 990. Two Knauer columns were used in series, each 120 mm long and 4 mm in diameter. The stationary phase was SiO<sub>2</sub> with butyl groups on the surface (Nucleosil 500 C4 from Machery and Nagel in the first column and Nucleosil 1000 C4 in the second one). Nucleosil 500 and 1000 were also tried; the results with these more polar columns were less satisfactory.

The mobile phase was an aqueous solution of  $1 \times 10^{-3}$  M Cd(ClO<sub>4</sub>)<sub>2</sub> (Ventron) and  $1 \times 10^{-3}$  M sodium hexametaphosphate (Riedel de Haen). However, the latter mainly consisted of polyphosphates of different chain lengths; the molarities given refer to the formula (NaPO<sub>3</sub>)<sub>6</sub>. The flow rate was 0.5 mL/min, and the injected volume was 10  $\mu$ L. The spectra were taken and stored with an interval time of 1 s. To obtain size distribution curves, the chromatograms recorded at 250 nm were processed by using a Trivector chromatography data system, type Trilab-2000.

The preparation of the colloidal solution of various mean sizes has been described previously.<sup>2,4</sup> To prepare a sample for electron microscopy, a drop of the colloidal solution was applied for 30 s to a copper mesh covered with a carbon film and subsequently removed with a paper tip. Adhesion of the particles was promoted by exposing the carbon film to a glow discharge prior to this procedure.

## Results and Discussion

**Calibration.** The calibration of the column was made with 11 CdS samples of different mean particle size. The chromatograms of four samples, taken at 250 nm, are shown in Figure 1. They had a rather narrow size distribution, as can also be seen from the electron microscopic pictures in Figure 2. Particles of different size have a light absorption proportional to the cubic power of radius  $r$ . The mass weighted radius

$$\bar{r} = \sum n_i r_i^4 / \sum n_i r_i^3 \quad (1)$$

was calculated from the electron micrographs for each calibration sample. In Figure 3 the logarithmus of  $\bar{r}$  is plotted versus retention time. A linear curve resulted, as was observed previously in our experiments on chromatography at normal pressure.<sup>2</sup> Such a linear relationship between  $\log \bar{r}$  and retention time is also known from exclusion chromatography of polymers.<sup>7</sup>

With the calibration curve, size distributions of unknown samples can be calculated. Two CdS samples were investigated, i.e., sample  $\alpha$ , containing small particles with a relatively narrow size distribution around 50 Å, and sample  $\beta$ , having larger particles with a somewhat broader distribution around 80 Å. The size distributions were measured by electron microscopy and converted into mass distributions by weighing each size with the factor  $r^3$ . Figure 4 also contains the mass distribution as derived from the chromatograms. In this procedure the differential and integral distributions of Figure 5 were first calculated, from which the histograms in Figure 4 resulted. It can be seen that the histograms obtained by the two methods agree very well. Once a calibration curve and a suitable

(1) Fischer, Ch.-H.; Weller, H.; Fojtik, A.; Lume-Pereira, C.; Janata, E.; Henglein, A. *Ber. Bunsen-Ges. Phys. Chem.* 1986, 90, 46-49.

(2) Fischer, Ch.-H.; Lilie, J.; Weller, H.; Katsikas, L.; Henglein, A. *Ber. Bunsen-Ges. Phys. Chem.* 1989, 93, 61-64.

(3) (a) Henglein, A. *Top. Curr. Chem.* 1988, 143, 113-180. (b) Kalyanasundaram, K.; Grätzel, M. *Chemistry and Physics of Solid Surfaces*. V.; Vanselow, R.; Howe, R., Eds.; Springer-Verlag: Berlin, New York, 1984. (c) Fendler, J. H. *J. Phys. Chem.* 1985, 89, 2730-2740. (d) Thomas, J. K. *J. Phys. Chem.* 1987, 91, 267-276.

(4) Spanhel, L.; Haase, M.; Weller, H.; Henglein, A. *J. Am. Chem. Soc.* 1987, 109, 5649-5655 and references therein.

(5) (a) Fojtik, A.; Weller, H.; Koch, U.; Henglein, A. *Ber. Bunsen-Ges. Phys. Chem.* 1984, 88, 969-977. (b) Brus, L. *J. Chem. Phys.* 1983, 79, 5566-5571. (c) Brus, L. *J. Phys. Chem.* 1986, 90, 2555-2560.

(6) (a) Henglein, A.; Kumar, A.; Janata, E.; Weller, H. *Chem. Phys. Lett.* 1986, 132, 133-136. (b) Wang, Y.; Mahler, W. *Opt. Commun.* 1987, 61, 233-236.

(7) Determann, H. *Gelchromatographie*; Springer-Verlag: Berlin, New York, 1967; p 115.

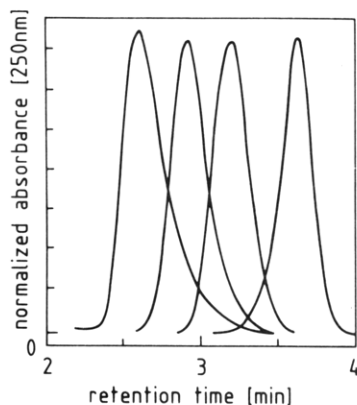


**Figure 1.** Chromatograms of a few CdS samples used for calibration.

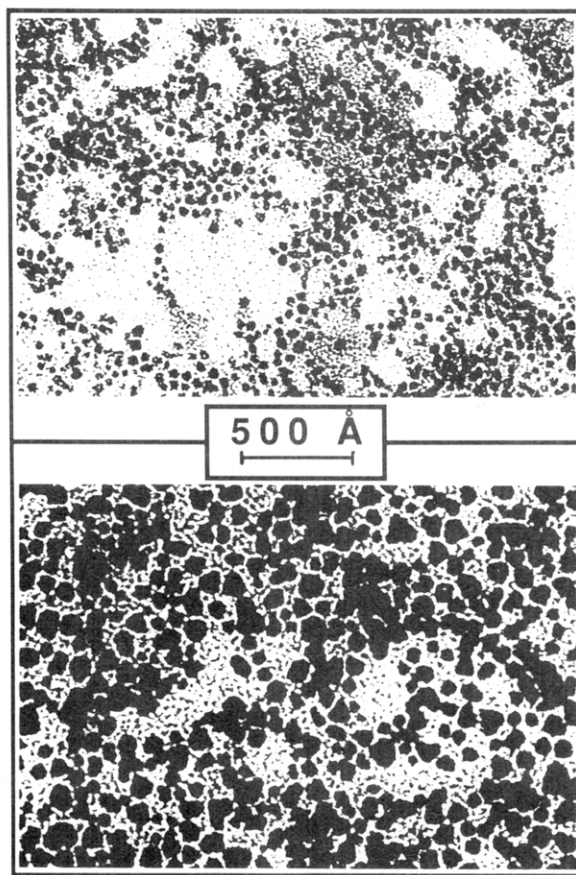


**Figure 2.** Electron microscopic pictures of two CdS samples used for calibration.

computer program exist, the size distribution of a colloidal solution can be obtained within minutes, a method much faster than the more time consuming electron microscopy. The precision of the method is better than 6% with respect to the determination of  $r$  as calculated from the observed scattering of the data.

**Structured Size Distributions: "Magic" Agglomeration Numbers.** Very small particles of CdS often have several maxima in the absorption spectrum, the origin of which is not yet fully understood. They could be interpreted as optical transitions to the various excited states in the particles, as small particles do not have a conduction band with a high density of states but a term scheme resembling that of a molecule (size quantization effect).<sup>5</sup> On the other hand, the maxima could arise when a sample has a structured size distribution, i.e., when certain agglomeration numbers are more abundant than adjacent

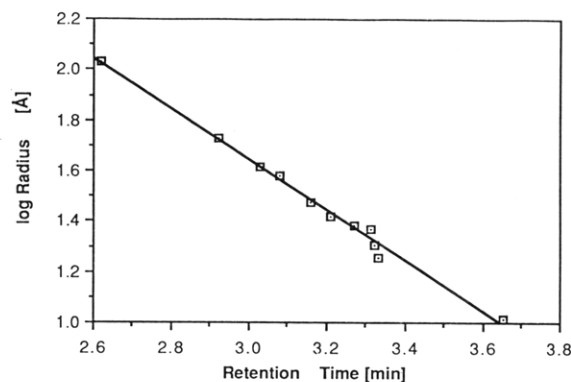


**Figure 3.** Calibration curve obtained by using 11 CdS samples, the histograms of which were measured by electron microscopy.

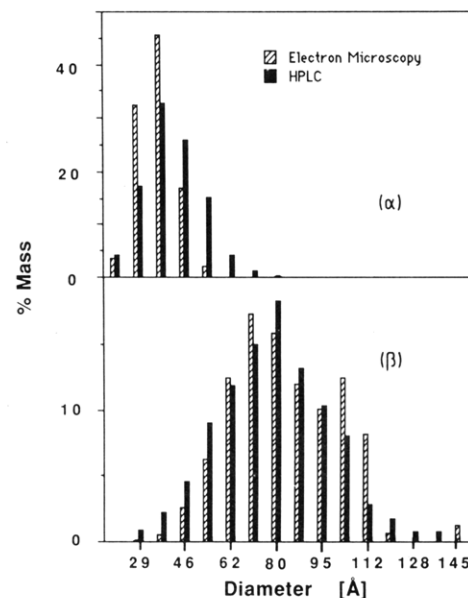


**Figure 4.** Mass distributions of two unknown CdS samples,  $\alpha$  and  $\beta$ , obtained by electron microscopy and by chromatography.

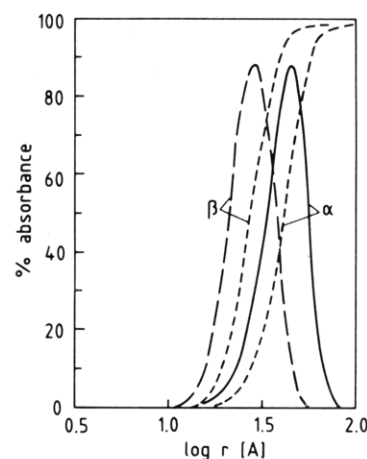


**Figure 5.** Integral and differential size distributions of the two CdS samples,  $\alpha$  and  $\beta$ , as derived from the chromatograms.

ones ("magic" numbers). A maximum would then correspond to the optical transition to the first excited state, which has most of the oscillator strength, in particles of different size.

In Figure 6 it is demonstrated how chromatography can be used to solve this problem. The insets of the diagrams show chromatograms of two CdS samples. These chromatograms show that the samples had structured size distributions. The particles in the upper diagram were

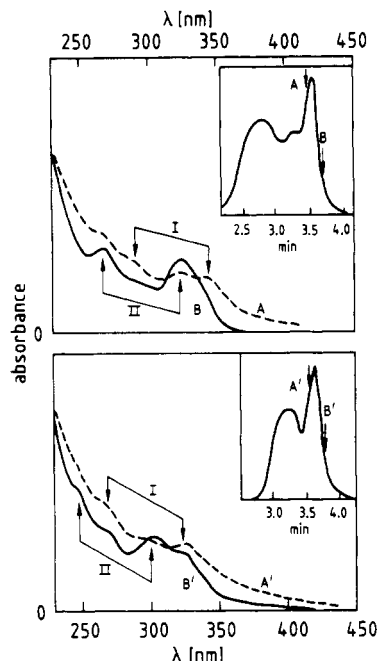


**Figure 6.** Absorption spectra of two fractions of CdS samples. The insets show the chromatograms of the samples.

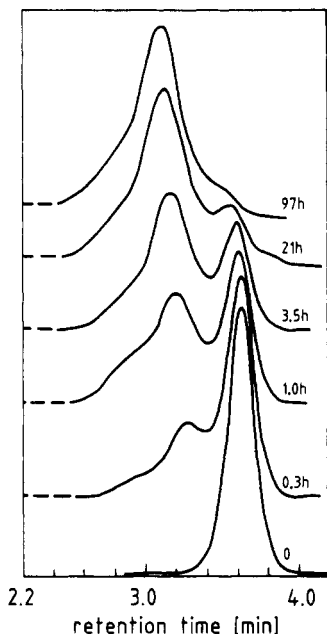


**Figure 7.** Thermal aging of small CdS particles. Chromatogram after different aging times. Dashed line: zero line of spectrum.

larger than the particles in the lower one.

The absorption spectra A and B, or A' and B', are shown; they were taken from the respective fractions A, B, A', and B' in the chromatograms. Fraction A had four weak maxima in the absorption spectrum. In fraction B, which contained smaller particles (although the separation is not complete), the first maximum is very weak as compared to fraction A, the second maximum is enhanced, the third maximum weaker again, and the fourth increased. Maxima which simultaneously increase or decrease when going from one fraction to the other are attributed to the same particle size. We thus reach the conclusion that the CdS sample in the upper part of Figure 6 contains at least two magic agglomeration numbers. For each of these a pair of maxima exists, the pairs being designated I and II in the figure. Within these pairs, the maximum of longer wavelength is attributed to the optical transition to the

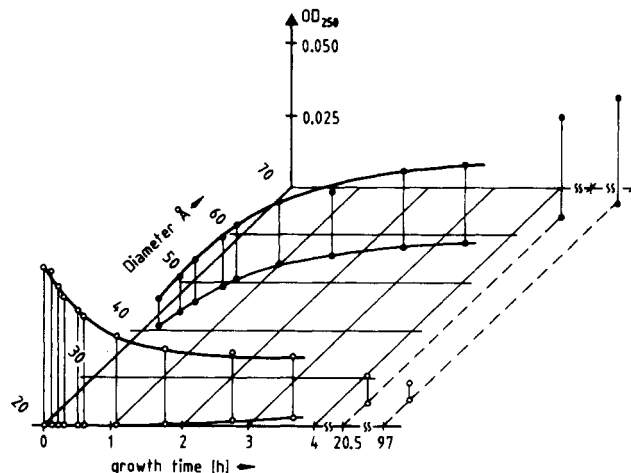


**Figure 8.** Three-dimensional diagram showing the height of the peaks in the chromatograms and the corresponding diameters as functions of time.

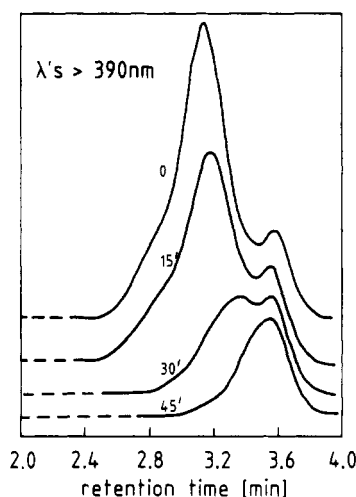


**Figure 9.** Chromatogram of a CdS sample at various times of illumination with  $\lambda > 390$  nm. Dashed line: zero line of spectrum.

first and the maximum at shorter wavelength to the second excitation level in these particles. A similar situation exists in the lower diagram of Figure 6.

**Particle Growth.** The chromatogram of a CdS sample initially containing very small particles is shown in Figure 7 at various times of aging at 20 °C. The peak at time zero appeared at a retention time of 3.63 min. During the growth, this peak becomes smaller and very slightly shifts to shorter retention times (larger particle size). However, the main effect consists in the formation and growth of a new peak at about 3.0 min, this peak moving rapidly to shorter retentions with increasing aging time.

From these chromatograms, the three-dimensional diagram of Figure 8 was constructed, which shows how the height and the diameter of the peaks of the two distributions change with time. One recognizes in the foreground the decrease in concentration (optical absorption at 250 nm where CdS particles have the same absorption coefficient regardless their size) of the small particles of the initial distribution. Further behind, one sees the increase in the concentration of significantly larger particles in the new distribution. While the size in the original distribution very slowly increases with time, there is a more rapid increase in size of the second distribution.

Particles can grow via Ostwald ripening or via combination. In the case of Ostwald ripening one expects a gradual increase in size and in the case of combination a rather sudden increase in the beginning of growth. The

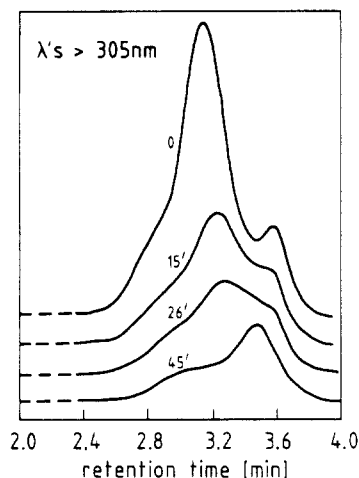
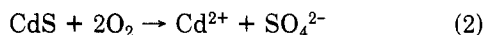


**Figure 10.** Chromatogram of a CdS sample at various times of illumination with  $\lambda > 305$  nm. Dashed line: zero line of spectrum.

shifts of the peaks of the initial and final distribution are probably due to Ostwald ripening. The rather fast jump from one distribution to the other is explained by particle combination. This latter contribution to particle growth is the dominating mechanism in the beginning.

**Photodissolution of Particles.** When a colloidal CdS solution is illuminated under air, a dissolution of the colloidal particles takes place, the overall process being



During the dissolution the particles become smaller, and this can be recognized from the accompanying changes in the shape of the absorption spectrum.<sup>3a</sup> More details,

however, can be recognized by HPLC. In Figures 9 and 10 chromatograms at different times of illumination are shown. The light source was a xenon lamp. In Figure 9, the light was passed through a 390-nm filter; in Figure 10 a 305-nm filter was used.

As the amount of CdS decreases during illumination, the area under the curves in the two figures becomes smaller with increasing time. The CdS sample used had two size distributions, as can be recognized from the two maxima in the chromatogram. Illumination with light of wavelengths greater than 390 nm (Figure 9) causes a decrease in the first maximum of the chromatogram, which is due to larger particles absorbing at longer wavelengths. The smaller particles do not have significant absorption above 390 nm, and they are therefore not much damaged. The peak of the size distribution of the larger particles gradually shifts to longer retention times (smaller particle sizes).

When light with wavelengths above 305 nm is used (Figure 10), the small particles are also affected, although to a lesser degree than the larger ones. It is noted that the peak of the distribution of the smaller particles does not move to longer but to shorter retention times. The reason for this lies in the fact that small particles are not only consumed but also formed from larger ones during the illumination. It was not intended to undertake a more thorough investigation of the complex kinetics of photodissolution, as the purpose of this paper consists in demonstrating the usefulness of HPLC in small-particle investigations.

**Acknowledgment.** We thank U. Michalczyk for assistance in the laboratory work.

**Registry No.** CdS, 1306-23-6.

## Motions of Droplets on Solid Surfaces Induced by Chemical or Thermal Gradients

F. Brochard

Université Pierre & Marie Curie, SRI-Bât Chimie Physique, 11, rue Pierre & Marie Curie, 75231 Paris, Cedex 05, France

Received May 11, 1988. In Final Form: November 14, 1988

The equilibrium shape of a liquid droplet, lying on a horizontal solid surface, is controlled by the spreading coefficient  $S$ . For partial wetting ( $S < 0$ ), a drop smaller than the Laplace length  $\kappa^{-1}$  forms a spherical cap, while a drop much larger than  $\kappa^{-1}$  forms a thick "pancake". For complete wetting, the liquid spreads as a very thin pancake. If  $S$  is nonuniform, all these structures are set into motion. We discuss this in the limit of small gradients ( $\nabla S \rightarrow 0$ ) for two cases: (I)  $\nabla S$  is obtained via a chemical treatment of the solid surface; here we predict that the droplets, or pancakes, move in the direction of *lower* surface energies. (II)  $\nabla S$  is the consequence of a temperature gradient  $\nabla T$ . The Marangoni effect plays an important role. If the surface tension  $\gamma$  of the liquid is temperature dependent, while all other interfacial tensions are not, we predict motions toward the regions of *higher* surface energies.

### I. Introduction

A droplet lying on a horizontal solid surface moves under a horizontal temperature gradient  $\nabla T$ : this motion has been qualitatively observed for a long time,<sup>1</sup> but no quantitative study is available. On the theoretical side, the problem is somewhat complex.

The liquid/air surface tension  $\gamma$  is temperature dependent; thus  $\nabla T$  induces a  $\nabla \gamma$ , and this induces a Mar-

angoni flow<sup>2</sup> in the droplet. The other two surface tensions,  $\gamma_{\text{SO}}$  and  $\gamma_{\text{SL}}$  (solid/air and solid/liquid), may also be  $T$  dependent. This has two main consequences.

(i) A small "Soret velocity"<sup>3</sup>  $V_S$  is induced in the liquid just above the liquid surface.  $V_S$  is linear in  $\nabla T$ . P. G.

(2) Marangoni, G. G. M. *Sull'espansione delle gocce di un liquido galleggiante sulla superficie di altro liquido*; Pavia tip Fusi: Agosto, 1865. Marangoni, G. G. M. *Ann. Phys. (Poggendorf)* 1871, 143-337.

(3) de Groot, S. *L'effet Soret*; North-Holland: Amsterdam, 1945. de Groot, S.; Mazur, P. *Nonequilibrium thermodynamics*; North-Holland: Amsterdam, 1962. de Gennes, P.-G. *C. R. Acad. Sci. Paris* 1982, 295-959.

(1) Bouasse, H. *Capillarité et phénomènes superficiels*; Delagrave: Paris, 1924.